Available online at www.sciencedirect.com
SCIENCE DIRECT
Journal of Photochemistry and Photobiology A: Chemistry 179 (2006) 200–212
Journal of Photochemistry and Photobiology A:Chemistry
www.elsevier.com/locate/jphotochem

Beneficial effects of photo-inactive titanium dioxide specimens on plasmid DNA, human cells and yeast cells exposed to UVA/UVB simulated sunlight☆

Nick Serpone[a,*,1], Angela Salinaro, Satoshi Horikoshi[b], Hisao Hidaka[b]

[a] *Dipartimento di Chimica Organica, Universita di Pavia, Via Taramelli 10, Pavia 27100, PV, Italy*
[b] *Global Environment Science Center, Meisei University, 2-1-1 Hodokubo, Hino, Tokyo 191-8516, Japan*

Received 9 May 2005; received in revised form 21 July 2005; accepted 12 August 2005
Available online 15 September 2005

Abstract

Photoactive TiO_2 specimens extracted from commercial sunscreen lotions had been shown earlier [R. Dunford, A. Salinaro, L. Cai, N. Serpone, S. Horikoshi, H. Hidaka, J. Knowland, FEBS Lett. 418 (1997) 87] to cause damage to both DNA plasmids in vitro and to whole human skin cells in cultures by photoproduced $^{\bullet}OH$ radicals. This article reports on the effects of TiO_2 specimens, whose particle surface was modified by a thermally assisted procedure to produce TiO_2 specimens of considerably reduced photo-activity. Deactivation of the photocatalytic activity of TiO_2 impacts on the kinetics of photooxidation of phenol and has a significant effect in diminishing, if not suppressing completely, damage caused to DNA plasmids, to human cells, and to yeast cells compared to non-modified specimens exposed to UVB/UVA simulated solar radiation. Photo-inactive TiO_2 could be beneficial in sunscreen formulations and in polymer blends, since they also completely retain their UVB/UVA absorption/scattering (screening) characteristics. Synergistic effects of titania specimens with an organic sunscreen active agent (Padimate-O) on DNA plasmids and the survival of yeast cells in the presence of titanium dioxide, and in the presence of such UV filters as Padimate-O and Parsol 1789 (i.e., avobenzone) under UV irradiation are reported.

Keywords: Titanium dioxide; UV physical filter; Plasmid DNA; Yeast cells; Human cells; Padimate-O; Parsol 1789; Deactivation of photo-activity

1. Introduction

Mineral compounds are used extensively in such cosmetics as foundations, powders, eye shadows and pencils. Related to this, titanium dioxide (TiO_2) was reported as a sunscreen agent as long ago as 1952 [1]. The required feature of metal-oxide UV filters is to block the solar UV light from penetrating the skin over the whole UVA/UVB range (290–400 nm) through reflection, scattering and absorption, which in turn are determined by the intrinsic refractive index, the size of the particles, dispersion in the appropriate medium, and by the film thickness. The ability of metal oxides to act as UV filters in sunscreen lotions is determined by two major characteristics: their reflecting property and their cosmetic acceptability. Particle sizes in the range 200–500 nm for a metal oxide such as TiO_2 (and ZnO) are best at reflecting visible light. However, such particles are opaque on the skin.

Cosmetic acceptability has required a decrease of the particle size. Addition of brown iron oxide (Fe_2O_3) pigments improves product appearance. So-called micronized (20–50 nm) metal-oxide particles are used in cosmetic products [2], as they are easily incorporated into emulsions, are transparent to visible radiation, and reflection from the particle surface is minimal. Light attenuation by these smaller particles is due mostly to Rayleigh scattering and to significant absorption of UVB and UVA sunlight [3].

TiO_2 has been reported to be non-mutagenic and so could not impart damage to DNA [4]. However, this study failed to recognize the effects of sunlight on TiO_2 and on the particular

☆ Taken in part from the Ph.D. thesis of Angela Salinaro, Concordia University (2001), Montreal, Canada.

* Corresponding author. Tel.: +39 0382 98 78 35; fax: +39 0382 98 73 23.
E-mail addresses: nick.serpone@unipv.it, serpone@vax2.concordia.ca (N. Serpone).
[1] Professor Emeritus, Concordia University, Montreal, Que., Canada.

1010-6030/$ – see front matter © 2005 Elsevier B.V. All rights reserved.
doi:10.1016/j.jphotochem.2005.08.017

nature of TiO_2 in actual use in sunscreen products. This is especially significant because sunscreen TiO_2 is often coated with such compounds as $Al(OH)_3$, alumina, silica and zirconia, which in some instances enhances the photocatalytic activity of TiO_2 [5–7].

Titania is easily prepared by hydrolysis of a titanium(IV) precursor to give anatase and rutile, and some quantity of an amorphous phase. On contact with water (or water moisture) the surface of the nanocrystallites becomes highly hydroxylated, which strongly influences photo-catalyzed redox reactions taking place at the nanoparticle/solution or nanoparticle/gas interfaces. The titania surface has acid/base characteristics displaying two pK_a's (pK_{a_1} ~3; pK_{a_2} ~9) such that at pHs below the point of zero charge (pzc) the surface is positively charged, is neutral at the pzc, and negative at pHs greater than pzc. This change in the surface characteristic can influence adsorption/desorption of substrates coming into contact with TiO_2 particles and thus impact on the kinetics and mechanistic details of photocatalyzed reactions. The pzc of anatase titania is typically ca. 5.8 [8]; for the mixed phase Degussa P-25 titania sample (ca. 80% anatase, 20% rutile), the pzc ranges between 5.5 and 6.0 [9].

Photophysical events that occur after UVA/UVB illumination of TiO_2 (band-gap energy of anatase, 3.2 eV; for rutile, 3.0 eV) and subsequent formation of electron/hole pairs are many and very complex. Following electron/hole separation, the two charge carriers migrate to the surface through diffusion and drift [10], in competition with a multitude of trapping and recombination events in the lattice bulk. At the surface, these carriers are poised to initiate redox chemistry with suitable pre-adsorbed acceptor and donor molecules in competition with recombination events to yield radiative and nonradiative emissions, and/or trapping of the charge carriers into shallow traps at lattice sites (e.g., anion vacancies, Ti^{4+}, and others). Thus, on absorption of UV light, titania particles yield superoxide radical anions ($O_2^{-\bullet}$) and hydroxyl radicals ($^\bullet$OH) that can initiate oxidations [11]. The photo-activity of TiO_2 is set by a complex combination of factors, the most critical of which appears to be the nature of the surface [12], a problem which is still under active debate and investigation [13]. Some of these otherwise complex photophysical events occurring in most metal oxides (e.g., ZrO_2, Sc_2O_3 and others) have been the object of active and systematic studies [14]. A complete picture of the photo-activity of TiO_2 and other metal oxides in contact with chemical and biological systems is now emerging.

Since the key to change the activity of metal-oxide photocatalyst surfaces hinges on the number and type of surface active sites [14], home-made TiO_2 colloids and TiO_2 specimens from various commercial sources have been modified to produce photo-inactive TiO_2 systems. Their photo-activity was probed using the photooxidation of phenol, along with damage to DNA plasmids in vitro, human cells and yeast cells (in cultures).

UV light irradiated TiO_2 sunscreen specimens extracted from sunscreen lotions were shown earlier [15] to produce single- and double-strand breaks on plasmid DNA, and on nuclei of whole human skin cells. In this regard, Huang et al. [16] noted that UVB/UVA-irradiated uncoated 10-nm TiO_2 particles induces oxidative damage to DNA leading to cell death that could be prevented in the presence of reactive oxygen scavengers. In related studies, Afaq et al. [17] reported that intratracheal exposure of rats to about 2 mg of uncoated small TiO_2 particles (<30 nm) led to lipid peroxidation and H_2O_2 production associated with enhancement of antioxidant enzyme activity and cytotoxicity to pulmonary alveolar macro-phages. Nakagawa et al. [18] showed that, under dark conditions, TiO_2 particles have no or else display only weak genotoxicity toward DNA; however, when irradiated with UV radiation from a solar simulator TiO_2 caused significant damage to DNA (comet assay). Clearly, the potential for DNA damage associated with using TiO_2 (and ZnO also) as a UV filter in suncare products cannot be underestimated. To cause damage to DNA in vivo, TiO_2 must penetrate the skin and most importantly the cell nucleus. Some inferences that TiO_2 does penetrate the skin have been reported [19–22], although the data were somewhat inconclusive [23]. In one study, X-ray microanalyses and scanning electron microscopy failed to reveal the presence of TiO_2 in deep layers of the skin [24]. Similarly, Dussert et al. [25] found no intercellular or intracellular penetration of TiO_2, although a time course of the penetration was not performed [23]. Contrary to these studies, however, others have recently found that TiO_2 particles do indeed enter the skin [26–29], and to the extent that TiO_2 also enters human cells [30], it is important to examine details of the possible consequences of TiO_2 (coated or otherwise, and present in most sunscreen lotions) on DNA.

To the extent that TiO_2 is photo-active and DNA damage on human skin has been shown to follow from photogenerated $^\bullet$OH radicals [15], it becomes imperative, therefore, to inactivate TiO_2. A full report on the thermally assisted inactivation of TiO_2 samples from several sources, and a full characterization of their properties will be reported elsewhere [31]. Our strategy has been to modify and examine TiO_2 samples using a variety of in vitro models. The goal is part of an ongoing effort to prepare titanium dioxide specimens that would be photocatalytically inactive, but that would nonetheless provide some form of protection against the damaging UV sunlight radiation.

This article explores the features of some ten or so photo-inactivated TiO_2 specimens that might find use in sunscreen lotions and polymer blends. Specifically, we examine the photo-activity, or lack thereof, of these specimens before and after modification using the well-characterized photooxidation of phenol. The present study also evaluates photo-induced damage to DNA caused by illuminated TiO_2 samples before and after modification. The plasmid-nicking assay examines single-strand and/or double-strand breaks inflicted on naked DNA in vitro and the extent of such damage (if any) by photo-inactive TiO_2. *Saccharomyces cerevisiae* yeast cells were employed to evaluate the toxicity of TiO_2 specimens. Keratinocyte human skin cells were used in vitro (comet assays) to establish whether any observed reaction on naked DNA occurred within the cellular environment. This single-cell gel electrophoresis assay is a sensitive technique with low detection limit (0.032 gy; 1 strand break per 2×10^{10} Da of DNA) [32], and provides a visual method for assessing DNA strand breaks in single cells.

2. Experimental

2.1. Materials and methods

2.1.1. Preparation of homemade titanium dioxide colloid specimens

Chemicals were of reagent grade quality; water was doubly distilled and deionized. Colloidal sols of TiO_2 were prepared either by a low-temperature controlled hydrolysis of $TiCl_4$ or by hydrolysis of Ti(i-PrO)$_4$, according to procedures reported by Lawless [12]. A typical preparation involved hydrolysis of doubly distilled titanium(IV) chloride (Aldrich), whereby 5.2 mL of $TiCl_4$ was added dropwise to 200 mL of doubly vacuum-distilled water (caution!). To obtain colloids of different particle size, the water and the $TiCl_4$ were maintained at temperatures given in Table 1, which also reports the corresponding particle diameter. The resulting mixture was dialyzed (Viscase membrane, presoaked for 24 h in distilled water and then thoroughly rinsed prior to use) against doubly distilled water (replaced several times) overnight to remove the HCl acid produced, leaving a suspension of ultrafine titanium dioxide. Further drying of the suspension left an ultrafine white powder. Small TiO_2 colloidal particles of ca. 2 nm dimensions (diameter) were produced when the above procedure was used with $TiCl_4$ maintained at −20 °C and water at 0 °C.

The other procedure [33] takes 125 mL of titanium(IV) isopropoxide (Aldrich) into a vigorously stirred 750 ml solution of doubly distilled water containing 5.25 mL of concentrated nitric acid. The solution was heated at ca 80 °C for 8–12 h under continuous agitation yielding a nearly transparent colloidal sol. Removal of solvent under vacuum at 100 °C gave an ultrafine powder of TiO_2 (labeled RA1B).

Home-made and several commercialized TiO_2 specimens (Degussa P25, Sachtleben Chemie Hombikat UV-100, Bayer rutile, Sargent Welch, Fluka, Aldrich rutile, Aldrich anatase, Baker & Adams, Tioxide Canada, and Strem Chemicals) were modified [31] to passivate the particle surface and to minimize, or altogether suppress, their photocatalytic activity. Modified (henceforth coded as RNA,where N is a number) and unaltered (RNB) TiO_2 specimens were characterized by the Brunauer–Emmett–Teller (BET) specific surface area using a YASA IONICS Co. Ltd. instrument, and by changes in surface acidity (loading, 2 g L^{-1}) in doubly distilled water. Diffuse reflectance spectra were recorded on a Shimadzu UV-265 spectrophotometer fitted with an integrating sphere reflectance unit.

Table 1
Effect of temperature of $TiCl_4$ and water on the preparation of TiO_2 of different particle size

Temperature of $TiCl_4$ (°C)	Temperature of water (°C)	Average particle diameter (nm)	Sample label
−20	0	2.3 ± 0.1	R20B
0	0	16 ± 2	R21B
24	24	28 ± 2	R22B

2.1.2. Photocatalyzed oxidation of phenol

The ability of the RNB and RNA TiO_2 specimens to photooxidize substrates through hydroxyl radicals was tested using phenol as the organic substrate under exposure to UV light. The temporal course of photodegradation of phenol was monitored by HPLC chromatography. Each TiO_2 specimen (loading, 0.05%, w/v; 58 mL phenol solution, 200 μM; air-equilibrated aqueous media; pH 5.5) was irradiated with either a solar simulator (Solarbox from COFOMEGRA Milano; light irradiance, 48 mW cm^{-2}; wavelengths, 310–400 nm) or a 1000-W Hg/Xe lamp (light irradiance, 32 mW cm^{-2}; wavelengths, 310–400 nm). One-milliliter aliquots of the irradiated dispersions were taken at various times and filtered trough a 0.1 μm membrane to remove the TiO_2 particles prior to HPLC analyses (isocratic procedure; ambient temperature; Waters 501 liquid chromatograph; Waters 441 detector; wavelength was 214 nm; HP 3396A recorder). The column was Waters BONDAPAK C-18 reverse phase; mobile phase was a 50:50 mixture of methanol (BDH Omnisolv grade) and distilled/deionized water.

2.1.3. Illumination of DNA in vitro (plasmid nicking assays)

2.1.3.1. Materials. Titanium dioxide specimens were tested by the plasmid nicking assay to detect inflicted DNA damage. Glass and plastic pipettes, and tubes were sterilized prior to use. Plasmids were from the circular *E. coli* pBluescript II SK^+ DNA (Stratagene; available from earlier studies [34]), prepared and analyzed on agarose gels by the method of Maniatis et al. [35]. This DNA exists in three different forms: supercoiled (S), relaxed (R) and linear (L). Finding the latter two forms indicates single- and double-strand breaks, respectively, of the S form of DNA. The intensity estimated for each form at various irradiation times is indicative of the extent of DNA damage. All chemicals used for the nicking assays were BDH analytical grade or equivalent. Water (milli-Q) was sterilized by autoclaving at 121 °C and 15 lbs in^{-2} (1.06×10^4 kg m^{-2}) pressures for 15 min prior to use.

2.1.3.2. Methodology. The concentration of DNA plasmids prior to use was determined using a Beckman DU62 spectrophotometer by measuring the absorbance of the DNA solution at 260 nm (A_{260}) and 280 nm (A_{280}). A ratio A_{260}/A_{280} greater than 1.8 yields a concentration of DNA (μg mL^{-1}) that is equal to $50 \times A_{260}$.

The as-prepared plasmid DNA was illuminated in the presence of different TiO_2 specimens. Each sample was sonicated and vortexed in water to obtain different final concentrations of TiO_2 (4, 2, 1 and 0.1%, w/v). A 25-μL aliquot of each specimen was added to 25 μL of plasmid (2–3 μg DNA) in 100 mM sodium phosphate solution (pH 7.4). The mixture was then illuminated as droplets (50 μL) on Eppendorf caps placed on a brass block embedded in ice to conserve the DNA at 0 °C. Illumination was carried out on a rotating plate to ensure homogeneous irradiation of the samples. Ten microliters of the sample were collected at appropriate time intervals. The irradiation source was a solar simulator [36] consisting of a 250-W ozone-free lamp, a WG 320 filter and a quartz lens; light irradiance between 300 and 400 nm was 12 mW cm^{-2}. A condensing lens was

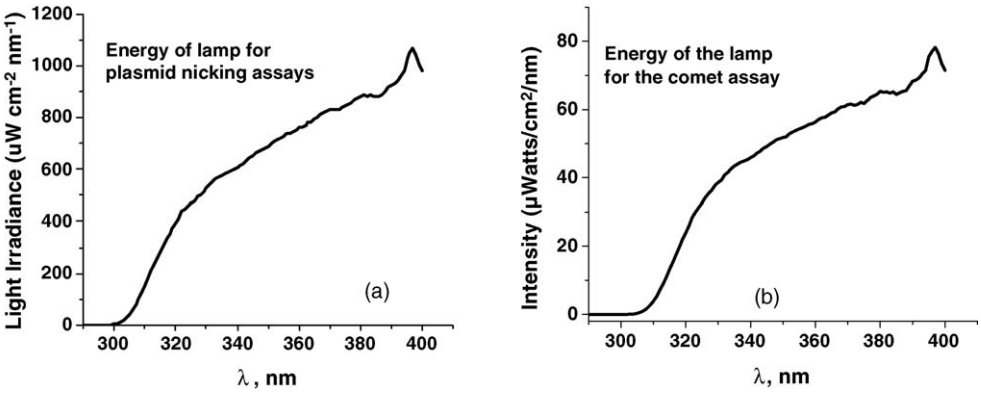

Fig. 1. Lamp spectral output (as light irradiance in units of $\mu W\,cm^{(2}\,nm^{(1}$ versus wavelength λ) used for: (a) plasmid nicking assays and (b) for comet assays as measured by a spectroradiometer.

placed between the lamp and the dichroic mirror to increase the light irradiance reaching the droplets. Measurement of the lamp output of the solar simulator (Fig. 1) was done using a cosine diffuser connected by a fiber optic cable to a double grating scanning spectroradiometer (Bentham Instruments Ltd., Reading, UK). Lamp output was constant for all experimental runs; bandwidth of monochromator was 1 nm; wavelength calibration was done using a CL6-H deuterium lamp previously calibrated against NPL reference lamps. Operation of the spectroradiometer was controlled using a Viglen desktop computer.

After illumination, the DNA was analyzed by Agarose gel electrophoresis, with the gels prepared according to Maniatis et al. [35]. They consisted of 1% (w/v) of agarose and 0.5× TBE buffer (44.5 mM Tris–HCl; pH 7.5; 44.5 mM boric acid and 1.25 mM of EDTA) heated until dissolved, then cast into a slab gel tray and allowed to set. Electrophoresis was performed in GNA 100 or GNA 200 gel tanks (Pharmacia) at $5\,V\,cm^{-1}$ for regular gels in 0.5× TBE buffer. The gels were subsequently incubated at ambient temperature for 45 min in 0.5× TBE buffer containing $0.3\,\mu g\,mL^{-1}$ ethidium bromide to stain the DNA. Stained DNA was viewed on a UV trans-illuminator (313 nm) and photographed on a Polaroid 665 positive/negative instant pack film. Relaxed forms of DNA were prepared by depurinating DNA plasmids at pH 4.8 in 25 mM sodium acetate and at 70 °C for 20 min. Cleavage was done at pH 8 with exonuclease III at 37 °C in a solution of 50 mM Tris–HCl and 5 mM of $CaCl_2$ (note that the Ca^{2+} ions inhibit exonuclease but not cleavage at apurinic sites), and 0.2 mM DTT. Linear standards were obtained by cutting the plasmid with EcoRI.

Appropriate photograph negatives of the plasmid nicking gels were scanned with a Bio-Rad model GS-670 imaging densitometer to compare the concentration of DNA in the three forms (supercoiled, relaxed and linear) present in each lane of the agarose gels. The reported graphical data represent the average of at least three experimental results.

2.1.4. Illumination of yeast Saccharomyces cerevisiae (droplet test)

2.1.4.1. Materials. All chemicals used for this test were BDH analytical grade or equivalent. Water (milli-Q), solid media, liquid media and solutions were all sterilized by autoclaving at 121 °C and at 15 lbs in.$^{-2}$ ($1.06 \times 10^4\,kg\,m^{-2}$) pressure for 15 min prior to use. Glass pipettes and Petri dishes were also sterilized by this method prior to use.

The yeast strain *S. cerevisiae* was of the XD83 type [34]. Yeast cells were grown in the dark in liquid YEPD medium (1 L of milli-Q Water, 10 g of yeast extract, 10 g of bactopeptone and 20 g of glucose) harvested in exponential phase overnight when the cell count (hemocytometer) was in the range $0.1–1 \times 10^7$ cells mL^{-1}.

2.1.4.2. Methodology. Yeast cells in the exponential phase were exposed to UV light in a 0.01 M sodium phosphate buffer (Petri dish; diameter, 60 mm; pH, 7.4; depth of cell suspension, ca. 2 mm). During light exposure, stirring ensured the homogeneity of the irradiation without changing the turbidity. The light source was the same solar simulator as in Fig. 1; light irradiance between 300 and 400 nm was $10\,mW\,cm^{-2}$. Titanium dioxide was tested by addition to the cell suspension to obtain a final concentration of 0.5% (w/v); TiO_2 was in direct contact with the cells. Samples were irradiated at various time intervals (0, 10, 20, 30 and 40 min). At each time point, a droplet (20 μL) was collected and loaded onto a Petri dish containing the solid media consisting of 10 g of yeast extract, 10 g of Bactopeptone, 20 g of D-glucose, and 20 g of Agar. Yeast cells that survived were noted after growth at 37 °C on a complete solid medium in a Petri dish. The droplet test gauged the potential toxicity of TiO_2 specimens on yeast cells by noting the yeast colonies that survived after each irradiation period. Various control experiments were performed to ensure the integrity of the yeast cells. In control experiments (no TiO_2), the cells were left in the dark for a period equal to the times of the irradiation experiment. In other control experiments, the cells were irradiated in the absence of TiO_2 to establish the mortality rate of yeast cells under UV radiation alone. Other control experiments were performed by adding the chemical (organic) sunscreen agent only, e.g., Padimate-O (50 μM) or Parsol 1789 (100 μM); these two chemical sunscreen filters were shown earlier to be genotoxic to yeast cells [36].

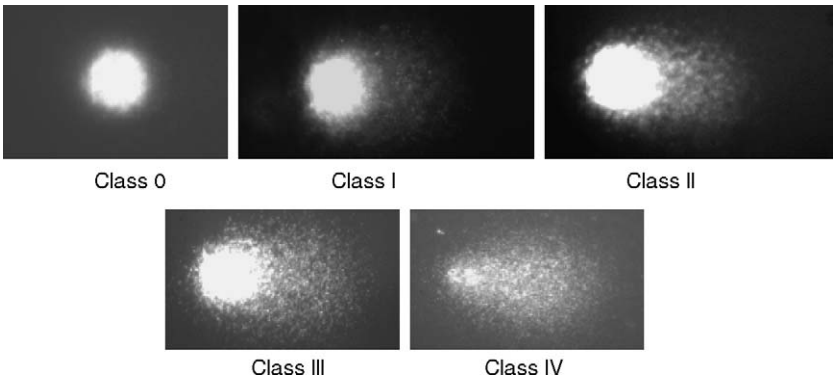

Fig. 2. Representation of the five main standard classes of comets.

2.1.5. Illumination of DNA in vitro (comet assays)

2.1.5.1. Materials. Comet assays were carried out by the procedure of Ostling and Johanson [37] as modified by Singh et al. [38]. Human cells were the human keratinocytes NCTC 2544 (Dr. Nigel Cridland; NRPB, UK), grown to confluent monolayers in NCTC media that consisted of 10% fetal calf serum and 1% penicillin and streptomycin. The flasks were incubated at 37 °C under an atmosphere of 5% CO_2. All chemicals and media were from Gibco BRL Life Technologies, UK.

The cells were harvested in a sterile hood, washed with a PBS solution (0.1 M sodium phosphate; pH 7.4; 0.1 M sodium dihydrogen phosphate; pH 7.4; 2.7 mM KCl; and 0.137 M NaCl) and a 1 mM EDTA solution, and then were treated with 2 mL of freshly prepared, filter sterile, 0.25% trypsin in PBS for 5 min at 37 °C to detach them from the base of the flasks. The cells were collected in a sterilin tube and centrifuged at 800 rpm for 5 min. The pellet of cells was resuspended in ice-cold PBS to give a final concentration of 2×10^6 cells mL^{-1}.

2.1.5.2. Methodology. The solar simulator was the same as in Fig. 1. For illuminations of whole cells, the condensing lens and the dichroic mirror used to increase the light irradiance in the plasmid nicking assays were excluded in the comet assays. The light irradiance was similar to that found under the stratum corneum on sunlight illumination [36]. Fig. 1b shows the characteristics of the lamp output measured spectroradiometrically.

Cells illuminated in the presence of TiO_2 were suspended in PBS; a drop (25 μL) was mixed with 25 μL of 0.025% (w/v) TiO_2 to give a final concentration of 0.0125% (w/v) titania in the drop. Ten-microliter samples were collected after 0, 20, 40 and 60 min illumination and were subsequently mixed with 75 μL of 0.8% low-gelling-temperature Agarose (Sigma) at 37 °C. Samples were immediately placed onto a 22 mm × 22 mm square of an Agarose-coated microscope slide, after which they were covered in a cell lysis solution consisting of 0.1 M EDTA, 0.001 M Tris–HCl (pH 7.5), 2.5 M NaCl, and 1% of Triton X-100 for 1 h at 4 °C in the dark. Slides were washed twice for 5 min at 4 °C in PBS, and then covered in alkaline unwinding solution (0.3 M NaOH, 1 mM of EDTA) and kept in the dark at 4 °C for 40 min, following which they were placed in an electrophoresis tank and covered in 0.003 M NaOH, and 0.1 mM EDTA at 4 °C. After the electrophoretic experiments, carried out at 0.67 V cm^{-1} for 25 min, the slides were neutralized in 0.4 M Tris–HCl (pH 7.4) and the nucleoids then stained with a solution of 0.01 mg mL^{-1} ethidium bromide.

The cells were classified visually (Zeiss fluorescence microscope; 100 comets counted per slide) into one of five categories (0, I, II, III and IV) according to appearance and length of the comet tail (Fig. 2). DNA damage was quantified by the total comet score (TCS) using the method of Reavy et al. [39]. In a group of 100 cells, the minimum score was obtained (Eq. (1)) when all the comets were of class 0 (TCS = 100 × 0 = 0) and the maximum was obtained when all the comets were of class IV (TCS = 100 × 4 = 400).

$$\mathrm{TCS} = [(N_{0\,\mathrm{class}} \times 0) + (N_{\mathrm{I\,class}} \times 1) + (N_{\mathrm{II\,class}} \times 2) + (N_{\mathrm{III\,class}} \times 3) + (N_{\mathrm{IV\,class}} \times 4)] \quad (1)$$

where N refers to the number of comets of a given class, and the numbers 0, 1, 2, 3 and 4 refer to the value given to the comet class.

2.2. Results and discussion

The specific surface areas of the hydrophilic TiO_2 specimens extracted from commercial sunscreen lotions examined earlier [15] and that caused single- and double-strand breaks in the DNA, ranged from 1.5 to 70 $m^2\,g^{-1}$. No clear correlation was found between specific surface areas and the rates of photodegradation of phenol, not unexpected since photo-activity is not solely governed by the surface area of the metal-oxide particles [14]. In the present context, other factors such as the anatase-rutile content, which also varied from 0 to 100% and 100 to 0%, the presence of coatings on the TiO_2 particles, and the presence of other modifiers also played a role in the divergence of the photo-activity displayed by these specimens. For instance, one specimen was more efficient in photodegrading phenol relative to others, yet it was predominantly rutile whose specific surface area was 35 $m^2\,g^{-1}$ and contained ZnO as a photo-active co-catalyst. Comparison with a standard pristine rutile specimen (surface area, 6.6 $m^2\,g^{-1}$) showed that the latter was photocatalytically more active toward phenol oxidation. Another TiO_2

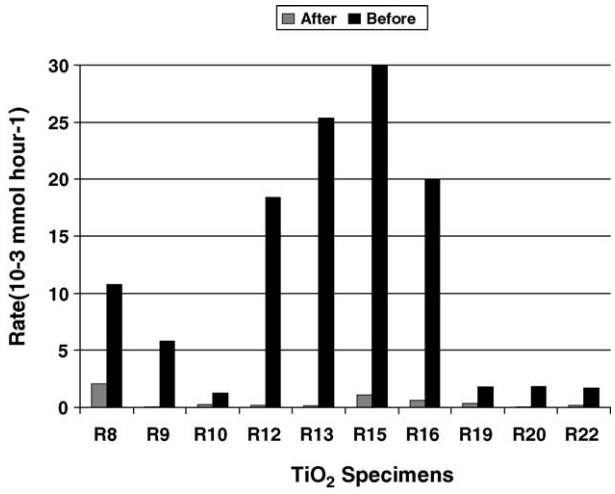

Fig. 3. Histogram summarizing the rates of photodegradation of phenol by several selected TiO_2 specimens before and after modification of the particle surface. The radiation source was the solar simulator (Solarbox).

specimen, coated with a layer of $Al(OH)_3$, was the least photo-active, yet it consisted of 50% rutile and 50% anatase and had a specific surface area of 3.1 $m^2\ g^{-1}$.

2.2.1. *Photo-activity of modified TiO_2 specimens toward the photooxidation of phenol*

Any decreased photo-activity of TiO_2 specimens must be, at least in part, the result of passivation of the catalyst surface. Histograms displayed in Fig. 3 illustrate the kinetic behavior of the specimens before (RNB) and after (RNA) inactivation for the photo-oxidative degradation of phenol, carried out using the solar simulator (COFOMEGRA Solarbox) as the UV radiation source. Results indicate that modification achieved the desired objective; that is, the rate of photodegradation of phenol was considerably and dramatically reduced for all specimens, albeit to different degrees. Specimen R15B was the most photo-active (Fig. 3). Note the dramatic decrease in photo-activity after passivation of the particle surface. Specimen R13 displayed the largest relative drop in the rate of photooxidation of phenol, followed by R15, R16 and R12 systems.

To be useful as inactive UV filters to screen, if not totally block, UVA and UVB sunlight radiation, modified TiO_2 specimens must retain their original UV absorption spectral characteristics. Fig. 4a and b illustrate the diffuse reflectance spectra of the R15 and R23 titania specimens, respectively, before and after passivation of the particle surface. In both cases, the original R15B and R23B samples block UVA/UVB radiation efficiently at all wavelengths below 400 nm. After surface passivation, the onset of attenuation of the incident radiation for the R15 sample was red-shifted to about 440 nm, thus making the modified samples even better sunlight UV filters. The corresponding R23 specimen showed only a slight red shift of the onset of attenuation after modification (Fig. 4b). For this latter sample, originally 100% rutile, passivation of the particle surface brings about no change in the specific surface area of the specimen (ca. 6 $m^2\ g^{-1}$).

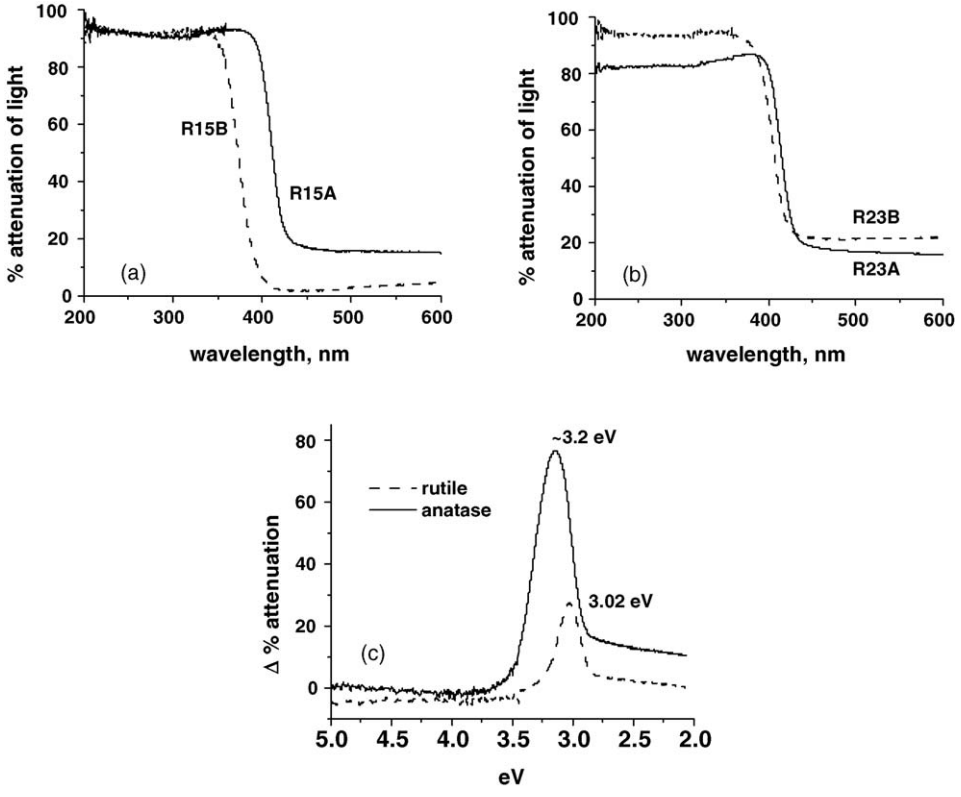

Fig. 4. Percent attenuation of light by the: (a) R15 titania specimens before and after surface modification; (b) percent light attenuation by the R23 titania specimen before and after surface modification; and (c) difference attenuation of light spectra for the R15 titania sample and for the R23 specimen before and after surface modification.

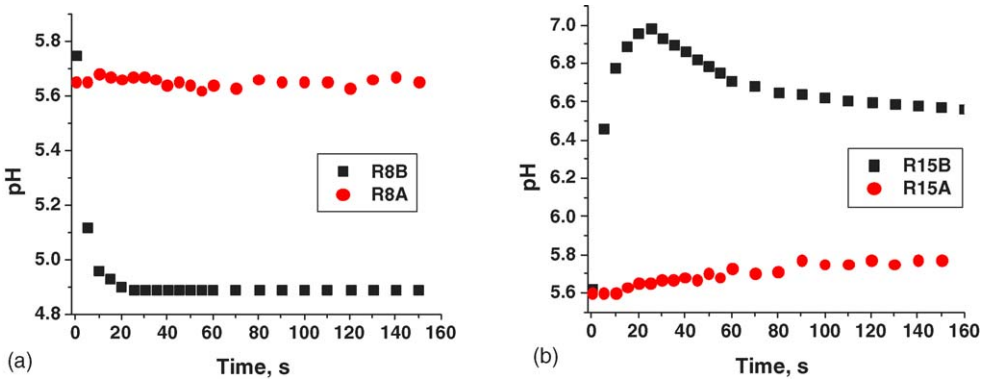

Fig. 5. Change in surface acidity of: (a) R8 and (b) R15 titania specimens before and after surface modification.

By contrast, passivation of the R8 titania specimen reduced the specific surface area from ∼55 to ca. 10 $m^2\,g^{-1}$. Fig. 4c illustrates the change-in-attenuation spectra (i.e., difference diffusion spectra) for R15 and for the R23 sample. The difference spectrum was maximal at 3.20 eV for R15 and 3.02 eV for the R23 TiO_2 specimen.

The hydrophilic characteristics of the specimens were also altered by surface passivation for many of the systems examined. This alteration is connected to surface changes that led to variations in either the number or the type of reactive centers present on the surface of the photocatalyst [13]. The change in hydrophilicity was confirmed by examining the change in surface acidity of the photocatalyst systems. The pH behavior of a 2 g L^{-1} dispersion of all TiO_2 specimens was altered with the modification as exemplified by the R8A and R8B specimens (Fig. 5a). Addition of the R8B TiO_2 specimen to water varied the pH from pH 5.7 to about pH 4.9 reaching this stable state after only a few minutes. This pH variation results from changes in adsorption/desorption equilibria established between the surface groups of TiO_2 and the aqueous phase as a result of variations of surface-active sites.

Fig. 5b depicts the pH changes for the R15B and R15A species. Addition of R15B to water rapidly led to an increase in pH from ca. 5.6 to a maximal pH of ca. 7.0 after 25 s, followed by a decrease to 6.6 reaching steady state after 60 s. By contrast, the R15A specimen displayed less dramatic pH changes increasing from initial pH 5.6 (pH of water) to stabilize at about pH 5.8 after 160 s. These pH changes confirm the complex nature of the particle surface, an issue well known to affect redox reactions (see e.g., ref. [40]).

Observation of a significant decrease in the rate of photodegradation of phenol suggests that modified titania specimens produced a considerable smaller number of $^{\bullet}OH$ radicals on UV irradiation. It is these radicals that are the primary cause of DNA damage [15], although a recent study [41] has shown that singlet oxygen, well known to be toxic to DNA, may also form on UV illumination of TiO_2 specimens. To the extent that the path leading to DNA damage is a complex process and species other than hydroxyl radicals may also be involved (e.g., H_2O_2 and $^1O_2$ [42]), the modified titanium dioxide specimens were also tested for possible damage to DNA plasmids and human cells using nicking assays and comet assays, and to yeast cells.

2.2.2. *Plasmid nicking assays*

Plasmid DNA was illuminated by UV light alone, and in the presence of modified and untreated TiO_2 specimens. Experiments were conducted under otherwise identical conditions of irradiation (calibrated solar simulator; Fig. 1a) for a 30-min period. During illumination by light alone the plasmids remained in their supercoiled form. Addition of TiO_2 caused a number of supercoiled plasmids of the circular, double-stranded DNA to be converted to the relaxed (R) and linear forms (L). Modified titanium dioxide specimens behaved differently. Damage (if any) caused by the modified specimens was considerably diminished, and was comparable to the damage inflicted by UV light alone acting on plasmid DNA (control experiment).

Fig. 6 displays an example of plasmid nicking assays, and illustrates the conversion of supercoiled DNA into its relaxed and linear forms for a variety of RNB TiO_2 specimens and for the corresponding modified RNA samples. When compared to the plasmid DNA control, all samples showed that modified UV-irradiated specimens caused far less damage to DNA than the untreated titania samples. A particular change in DNA plasmids, as evidenced by single- and double-strand breaks, was displayed by the RA1B and R8B titania specimens. Before modification, the RA1B colloids led to near complete disappearance of supercoiled plasmids after 20 min of illumination, whereas irradiation in the presence of modified RA1A only 15% of the supercoiled plasmids were damaged after 30 min. The R8B and R20B specimens cleaved plasmid DNA after only 10 min. The survival rate of plasmid DNA in the presence of treated R8A and R20A was greater than ∼90% (30 min). Specimen R22B completely destroyed all forms of the plasmids after 20 min of UVA/UVB irradiation. By contrast, the survival rate in the presence of the modified R22A specimen was ca. 80% after the 30-min irradiation period.

Fig. 7 summarizes results of nicking assays for plasmid DNA, and the effects that treated and untreated TiO_2 specimens, together with SiO_2 have on these plasmids. Overall results demonstrate that increase in concentration of modified TiO_2 (loading 0.05%, w/v) caused relatively no damage compared to the plasmid DNA control and to untreated rutile titania. Fig. 7a illustrates the effect of photo-inactive SiO_2 on DNA plasmids exposed to simulated UV sunlight. It was identical to those displayed by the modified R19A, R15A and R12A TiO_2 systems.

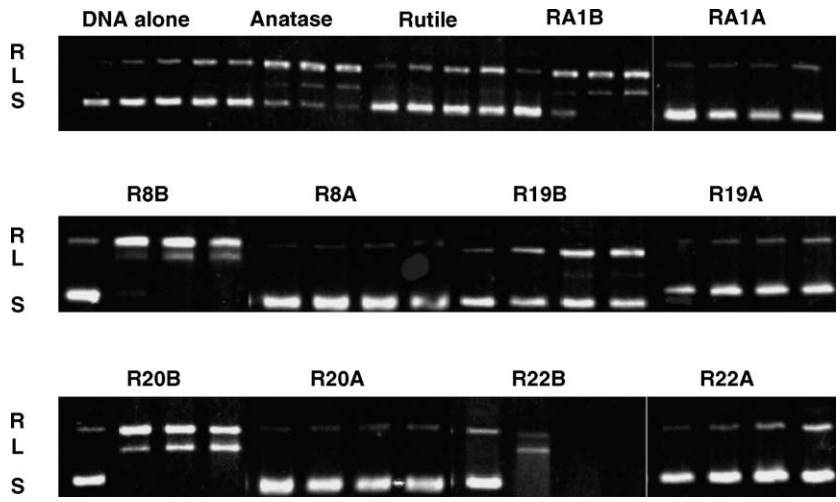

Fig. 6. Relaxation and migration of supercoiled (S), relaxed (R) and linear (L) forms of DNA plasmids caused by (top panel) UVA/UVB irradiation of DNA alone, in the presence of anatase, rutile and the selected TiO_2 specimens RA1B and RA1A specimens; (middle panel) in the presence of R8B, R8A, R19B and R19A samples; and (lower panel) with R20B, R20A, R22B and R22A titanium dioxide specimens. Irradiation times were 0, 10, 20 and 30 min. (titanium dioxide loading, 0.005%, w/v).

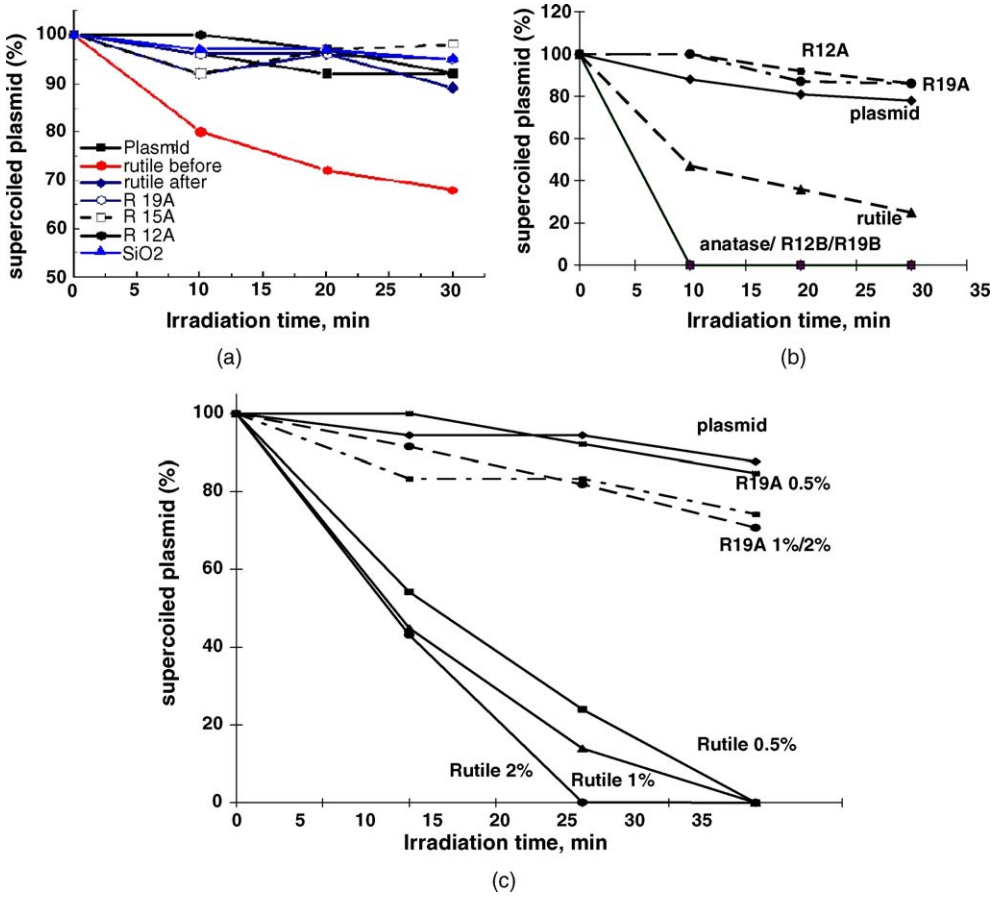

Fig. 7. (a) Plots showing the effect of 0.05% (w/v) of R19A, R15A and R12A titania specimens on plasmid DNA after surface modification, and comparison with the effects of rutile before and after modification, with silicon dioxide, and with a plasmid DNA control. (b) Effect of 0.5% (w/v) titanium dioxide specimens before (R12B and R19B) and after (R12A and R19A) surface passivation together with anatase and rutile titania specimens on the survival rate of supercoiled plasmid DNA. Plasmid DNA alone under UV irradiation is also displayed. (c) Concentration dependence of the effect of TiO_2 at various loadings (0.5%, 1% and 2%, w/v) on the survival rate of supercoiled plasmid DNA in contact with UV illuminated R19A and rutile specimens.

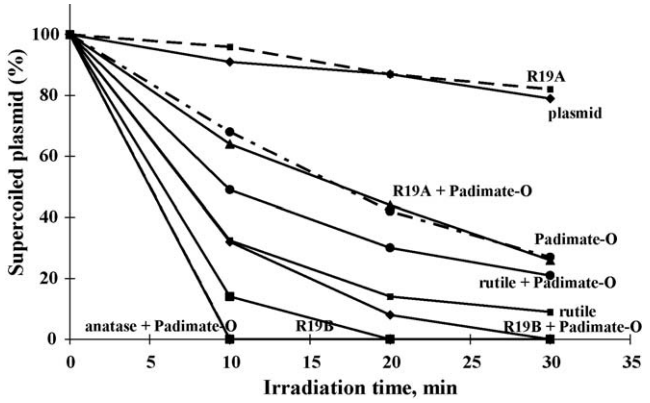

Fig. 8. Effect of 0.1% (w/v) titanium dioxide specimens (R19A, R19B, rutile and anatase) and Padimate-O (50 μM) alone and in combination on the survival rate of supercoiled plasmid DNA.

Fig. 7b displays a somewhat greater survival of supercoiled plasmids in the presence of R12A and R19A UV-irradiated specimens relative to DNA plasmids subjected to otherwise identical irradiation conditions. By comparison, both untreated rutile and anatase, together with R12B and R19B show considerable damage to supercoiled DNA plasmids, after only 10 min of UV irradiation for the latter three specimens. Conversion of supercoiled plasmids by rutile TiO_2 increased by about 30% for a tenfold increase in concentration (from 0.05% to 0.5%, w/v, respectively; Fig. 7a versus b).

The data shown in Fig. 7c confirm the effect of the concentration of TiO_2 on the survival rate of supercoiled plasmids for the rutile and R19A specimens when the concentration of titanium dioxide was increased from 0.5% to 1% to 2%, w/v. The concentration dependence is not monotonic above 0.5% w/v, however, because of an increase in light scattering by the larger number of TiO_2 particles at the higher concentrations, thereby attenuating the UV light absorbed by TiO_2. Nonetheless, the modified R19A specimen at 2% (w/v) loading inflicted very little damage to plasmid DNA. Other TiO_2 specimens showed similar behavior.

Fig. 8 illustrates the low (photo)activity and low damaging effect of the R19A sample compared to either the R19B (before modification) or to the Padimate-O sample, a well known UVB chemical sunscreen active agent used in some commercial formulations. The TiO_2 specimen R19A was completely inactive and protected DNA from the harmful effects of UV radiation. Addition of Padimate-O to DNA plasmids, however, caused considerable damage leading to a near 70% disappearance of supercoiled plasmids. Yet when R19A was also present with Padimate-O, the damage caused by the latter was unaffected by the inactive R19A specimen. The damage was even more pronounced on addition of the R19B sample, which caused complete destruction of the supercoiled plasmids after only 20 min of irradiation. Also shown is the synergy of the TiO_2 UV filter (R19) with Padimate-O since both R19B and Padimate-O attack DNA. When R19B and Padimate-O were combined they inflicted greater DNA damage than Padimate-O alone, but less than R19B. We infer that R19B photodegrades Padimate-O (as expected) and was so photo-active that it could inflict DNA damage and attack Padimate-O competitively. With rutile and Padimate-O present, the organic UV filter protected the DNA plasmids to some extent by scavenging $^{\bullet}OH$ radicals produced from irradiated rutile. However, Padimate-O was unable to protect plasmid DNA when anatase titania was also present in the mixture, because of the greater photo-activity of anatase (relative to rutile).

Padimate-O is photochemically unstable under UV illumination [43]. DNA species produced on irradiation of Padimate-O are unknown since plasmid nicking assays reveal only single- and double-strand breaks in supercoiled DNA caused principally by hydroxyl radicals [15]. It is possible that other radicals or some other reactive species may be formed, an issue that necessitates further examination on the photochemistry of organic sunscreen agents in synergy with TiO_2 systems [44].

2.2.3. TiO_2 and yeast cells

Yeast cells in the exponential phase were used because this is the phase of fast replication, and in this phase the cell walls are thinner and are more susceptible to penetration of TiO_2 particles into the cells. Initial experiments were also repeated for the stationary phase where the cell walls and the membrane are less porous. In this latter phase the modified TiO_2 specimens imparted no killing of yeast cells.

There are several possible mechanisms for cell killing by the photocatalytic process [45]. Yeast cells are made of a cell wall and a plasmalemma (membrane). The thick cell wall is as porous as a sieve with fairly large holes through which compounds can easily diffuse into the cells. Titanium dioxide can either destroy the cell wall or penetrate through the wall into the core of the yeast cell. Actions of the highly oxidizing $^{\bullet}OH$ radicals generated on the surface of illuminated TiO_2 particles are non-selective. Consequently, it is reasonable to expect the cell walls made of proteins to be oxidized first, followed by further $^{\bullet}OH$ radical attack on the membrane. When in contact with TiO_2, the cell walls become more permeable, ultimately leading to subsequent cell death. Some workers have reported evidence for disruption of cell walls, of cell membranes and leakage of the cell contents [46,47]. No electron microscopy evidence is available, however, to show that the cell walls are disrupted by TiO_2.

Fig. 9 illustrates results of the droplet test for the R9A and R9B specimens and compares them to the case when yeast cells were subjected to UV radiation alone and in the presence of the two organic sunscreen agents Padimate-O and Parsol 1789 (also known as avobenzone). In the dark, titanium dioxide had no effect on the survival rate of yeast cells. The effect of UV-irradiated TiO_2 was greater than that caused by UV light alone. In control experiments of yeast cells without titania, the cells survived after 40 min of irradiation with UVA/UVB simulated sunlight (Fig. 9A; note the number of yeast cells on the left column was twice that on the right column). The R9B titania specimen caused more kills than the treated R9A sample. Complete cell death occurred after only 10 min of illumination with R9B (Fig. 9B), whereas all the yeast cells survived even after 40 min of irradiation in the presence of R9A titania (Fig. 9C).

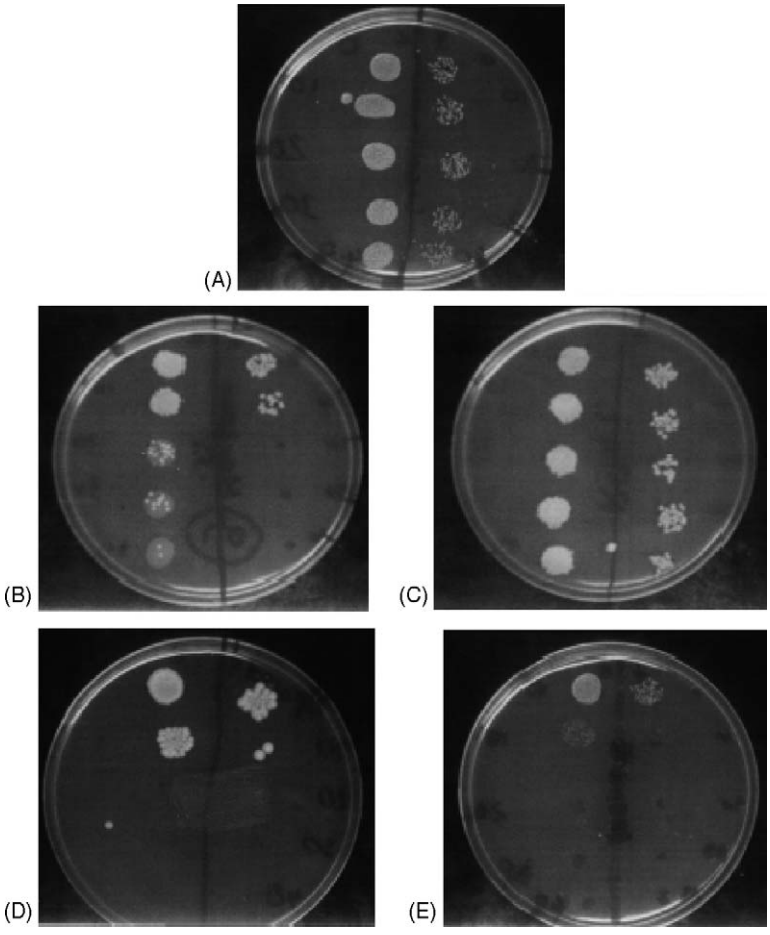

Fig. 9. Survival of yeast cells on UV illumination for 0, 10, 20, 30 and 40 min; from top to bottom in each Petri dish: (A) yeast cells alone; (B) R9B titania; (C) R9A titania; (D) Parsol 1789; and (E) Padimate-O. The Petri dish was divided into two parts to repeat the experiments. Note that the number of yeast cells on the left was twofold greater than the cells on the right.

The organic UVA sunscreen Parsol 1789 (Fig. 9D) and the UVB Padimate-O filter (Fig. 9E) were highly toxic to yeast cells causing cell death almost immediately upon UV irradiation.

Clearly, the modified RNA titania specimens are not toxic to yeast cells. We infer that the number of hydroxyl radicals produced was negligible for these specimens. Further studies on the photo-genotoxicity of titanium dioxide on yeast cells should be undertaken to determine the exact mechanism of kills of yeast cells and the genetic modification (if any) on the cells that may be caused by titanium dioxide under UV irradiation.

2.2.4. *Comet assays*

Several specimens were tested by the comet assay technique to further confirm DNA damage caused by illuminated TiO_2 on whole human skin cells in vitro. Treatment of keratinocyte cells with photo-activated titanium dioxide specimens produced comets after only 20 min of irradiation (Fig. 10 ; panel B). In the dark, TiO_2 specimens caused no damage to DNA. With increasing irradiation time, the number and nature of the comets increased; they tended to locate in the upper damage category.

Panel A of Fig. 10 illustrates the progress on illumination of keratinocyte cells (no TiO_2) for 0, 20, 40 and 60 min, and displays the extent of damage done to DNA by UVA/UVB radiation alone. Panel B depicts the damage caused on UV irradiation of the keratinocytes in the presence of R10B titania, also for the same time period. Clearly R10B imparted far more DNA damage than UV light alone in the absence of TiO_2. Compare, for example, the intensity of the comets at 60 min of irradiation for panels A and B. Panel C summarizes the results of UV illumination of the modified R10A titania specimen in the presence of keratinocytes under otherwise an identical irradiation period. Examination and comparison of the resulting comet after 60 min for the R10A specimen shows that this TiO_2 specimen caused very little damage to DNA relative to R10B. In fact, the nature of the comets also infers that R10A protects DNA to some extent against the harmful effects of UV radiation (compare panel C with panel A).

Fig. 11 summarizes the data from comet assays as three-dimensional bar charts. It shows the comet class or damage category (0–IV), the number of comets (out of 100 scored), and the irradiation time. The figure also illustrates an example of the effect(s) of modified TiO_2 specimens, and how this modification altered the number and category of the comets. Before modification, the R8B specimen (Fig. 11a) irradiated for only 20 min displayed some comets of category IV; the number of undamaged comets (category 0) was less than 10%. By

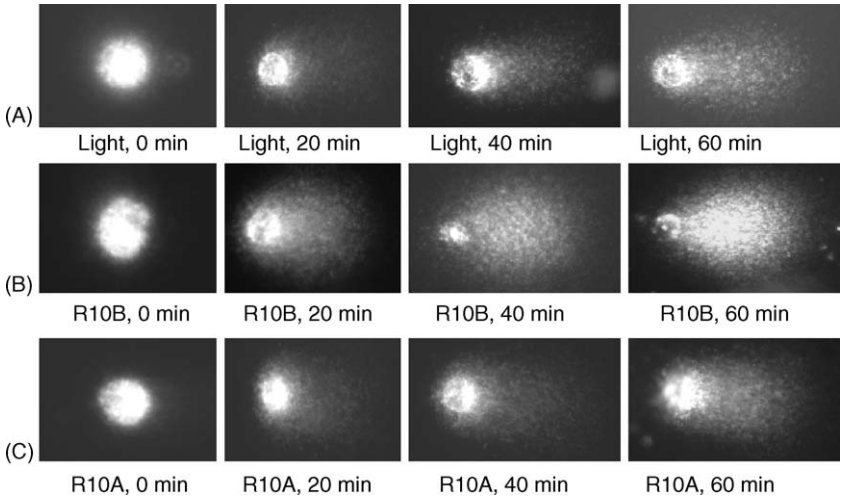

Fig. 10. Panels illustrating typical comets obtained from UV irradiation of plasmid DNA for 0, 20, 40 and 60 min alone (panel A) and in the presence of R10B titania (panel B). Panel C displays the contrasting effect of UV irradiation of plasmid DNA in the presence of the modified R10A titania specimen. (See text for more details).

contrast, the R8A titania sample (Fig. 11b), under the same irradiation conditions, caused less damage and no comets of category IV were evident; the number of comets of category II and III accounted for ca. 30% of total. In addition, treatment of keratinocyte cells with irradiated R8A caused nearly identical damage to that inflicted by UV light alone. The damage inflicted by rutile on the keratinocyte cells was less than that caused by R8B (ca. 80% anatase). Some comets of class IV also formed in the presence of rutile but only after 60 min of irradiation.

Fig. 11c and d illustrate the fate of keratinocyte cells when irradiated with UV light in the presence of TiO_2 specimens R10B and R10A (100% rutile). For these specimens the number and the class of comets produced differed from each other. In particular, the R10A specimen inflicted ca. 50% less damage than did R10B after 60 min of UV illumination.

Fig. 12 displays the total comet score (TCS) per 100 cells versus irradiation time. It demonstrates that TCS for anatase and for all non-modified specimens was rather high relative to the

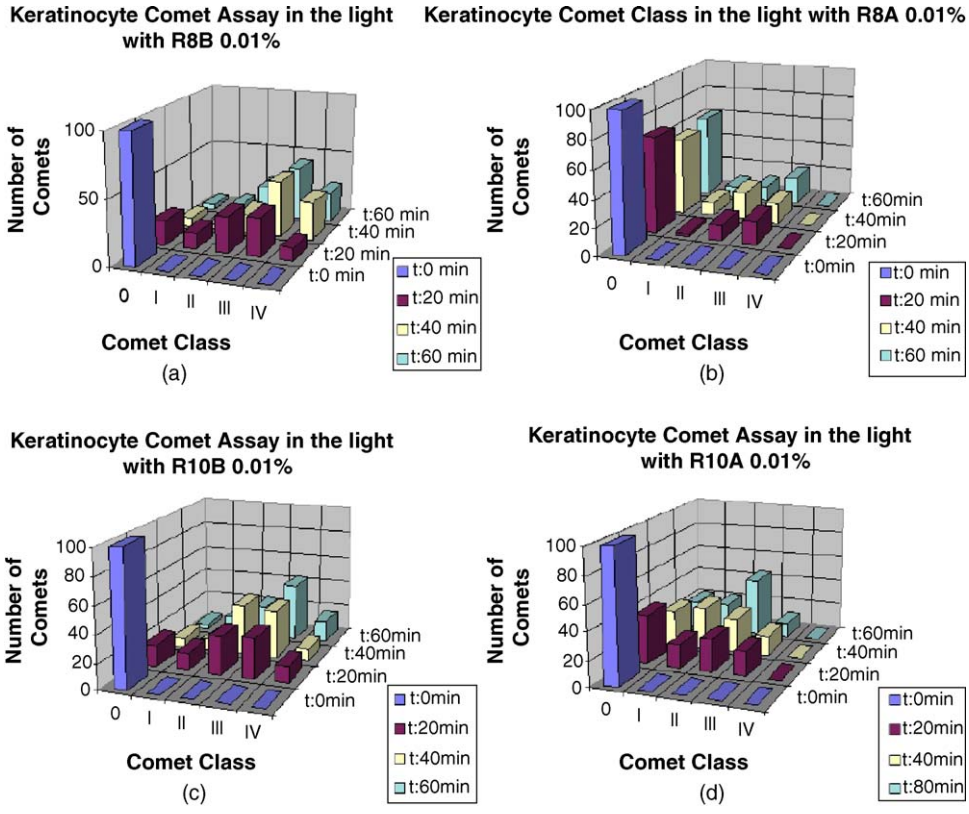

Fig. 11. Bar chart summarizes the results of UV-irradiating keratinocyte cells in the presence of: (a) R8B; (b) R8A; (c) R10B; and (d) R10A titania specimens.

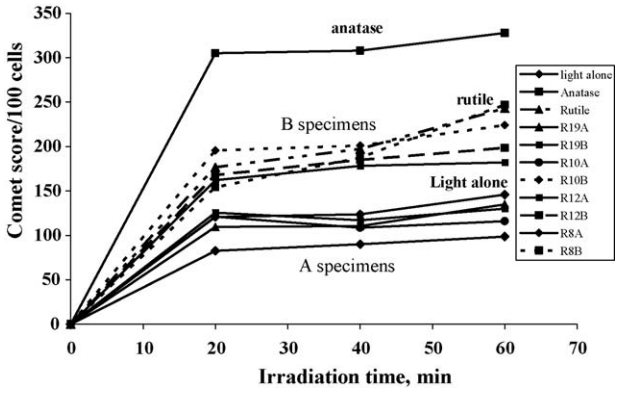

Fig. 12. Total comet score at various irradiation times for all the modified and unaltered TiO_2 specimens (see text for details).

total comet score obtained with irradiation by UV light alone (no TiO_2). By contrast, the modified RNA titania specimens yielded a total comet score below the TCS score on irradiation with UV light alone. The total comet score correlates with the number of lesions done on DNA that are induced by UV radiation [48].

2.3. Concluding remarks

The photo-activity of titania specimens extracted from sunscreen lotions and reported earlier [15] was the result of several factors, not least of which were the crystalline forms of TiO_2 and the specific surface area, as well as the number of active centers on the particle surface. Other parameters play important roles in the photo-activity of sunscreen TiO_2, namely the presence and amount of other physical filters (e.g., ZnO) and inorganic coatings such as $Al(OH)_3$. Our earlier results [15] showed that somehow the coating did not inactivate TiO_2, but in certain samples the activity was increased, in keeping with the findings of Anderson and Bard [6] who reported increased photo-activity of SiO_2-coated titanium dioxide.

Inactivated titania specimens dramatically reduce damage inflicted to DNA by harmful UV radiation and by irradiated titanium dioxide used as a UV filter in suncare products. Additional experiments should unravel the changes imparted on the particle surface upon passivation. Two such changes are possible: (i) a change in the number and nature of the active centers and (ii) a change in the number of OH^- groups on the particle surface [13]. Since adsorption/desorption events are important in photooxidations, any change in surface properties that affect adsorption/desorption characteristics of the specimens will also impact on the photo-activity of titanium dioxide.

Passivation of titanium dioxide particles has a significant influence on decreasing the extent of damage inflicted to plasmid DNA, whole human skin cells, and yeast cells relative to non-modified titania specimens when exposed to simulated sunlight UVA/UVB radiation. Passivated titania specimens caused no damage to these in vitro skin models. The modified specimens protected DNA from the harmful UVA/UVB radiation. By contrast, frequently used sunscreen active agents Parsol 1789 and Padimate-O caused considerable damage to yeast cells, confirming earlier work on plasmid DNA [49,50]. Further studies should ascertain which factors cause genotoxicity of sunscreen active agents, and how cells are modified as a result of the changes reported here.

Acknowledgments

We thank the Natural Sciences and Engineering Research Council of Canada for partial support of this work (to N.S.), and Dr. John Knowland (Department of Biochemistry, Oxford, UK) for many useful discussions on sunscreen chemical filters. Research in Pavia was sponsored by the Ministero dell'Istruzione, dell'Universita e della Ricerca (to N.S., MIUR, Roma) and in Tokyo by the Japanese Ministry of Education, Culture, Sports, Science and Technology (to H.H.). One of us (A.S.) is grateful to Dr. Knowland for his hospitality during two summer terms (1998 and 1999).

References

[1] D.W. Smithers, J.H. Wood, Lancet 1 (1952) 945.
[2] G.M. Murphy, Photodermatol. Photoimmunol. Photomed. 15 (1999) 34.
[3] N. Serpone, A. Salinaro, H. Hidaka, S. Horikoshi, J. Knowland, R. Dunford, in: J.M. Morehouse, R.E. Hogan (Eds.), Solar Engineering 1998, ASME, New York, 1998, pp. 287–298.
[4] Titanium Dioxide, IARC Monographs on the Evaluation of Carcinogenic Risks to Humans, 47 (1989) 307.
[5] M. Anpo, H. Nakaya, S. Kodama, Y. Kubokawa, J. Phys. Chem. 90 (1986) 1633.
[6] (a) C. Anderson, A.J. Bard, J. Phys. Chem. 99 (1995) 9882;
(b) C. Anderson, A.J. Bard, J. Phys. Chem. 101 (1997) 2611.
[7] Y. Xu, W. Zheng, W. Liu, J. Photochem. Photobiol. A: Chem. 122 (1999) 57.
[8] Y. Xu, M.A.A. Schoonen, Am. Miner. 85 (2000) 543.
[9] (a) E.A. Barringer, H.K. Bowen, Langmuir 1 (1985) 414;
(b) J. Moser, Ph.D. thesis, Ecole Polytechnique Federale de Lausanne, Lausanne, Switzerland, 1986.
[10] A. Emeline, A. Frolov, V. Ryanchuk, N. Serpone, J. Phys. Chem. B 107 (2003) 7109.
[11] N. Serpone, Kirk-Othmer Encyclopedia of Chemical Technology, vol.18, Wiley-Interscience, New York, 1996, pp. 820–837.
[12] D. Lawless, Ph.D. thesis, Concordia University, Montreal, Que., Canada, 1992.
[13] A.V. Emeline, N. Serpone, manuscript in preparation.
[14] (a) A.V. Emeline, N. Serpone, Chem. Phys. Lett. 345 (2001) 105;
(b) A.V. Emeline, A. Salinaro, N. Serpone, J. Phys. Chem. B 104 (2000) 11202;
(c) N.S. Andreev, A.V. Emeline, V.A. Khudnev, S.A. Polikhova, V.K. Ryabchuk, N. Serpone, Chem. Phys. Lett. 325 (2000) 288;
(d) A.V. Emeline, V.K. Ryabchuk, N. Serpone, J. Photochem. Photobiol. A: Chem. 133 (2000) 89;
(e) A.V. Emeline, G.N. Kuzmin, D. Purevdorj, V.K. Ryabchuk, N. Serpone, J. Phys. Chem. B 104 (2000) 2989;
(f) N. Serpone, A. Salinaro, A.V. Emeline, V. Ryabchuk, J. Photochem. Photobiol. A: Chem. 130 (2000) 83;
(g) A.V. Emeline, G.V. Kataeva, V.K. Ryabchuk, N. Serpone, J. Phys. Chem. 103 (1999) 9190;
(h) A.V. Emeline, E.V. Lobyntseva, V.K. Ryabchuck, N. Serpone, J. Phys. Chem. B 103 (1999) 1325;
(i) A.V. Emeline, V.K. Ryabchuck, N. Serpone, J. Phys. Chem. B 103 (1999) 1316;
(j) A.V. Emeline, A.V. Rudakova, V.K. Ryabchuk, N. Serpone, J. Phys. Chem. B 103 (1998) 10906;
(k) A.V. Emeline, S.V. Petrova, V.K. Ryabchuck, N. Serpone, Chem. Mater. 10 (1998) 3484;

(l) A.V. Emeline, G.V. Kataeva, A.S. Litke, A.F. Rudakova, V.K. Ryabchuck, N. Serpone, Langmuir 14 (1998) 5011.
[15] R. Dunford, A. Salinaro, L. Cai, N. Serpone, S. Horikoshi, H. Hidaka, J. Knowland, FEBS Lett. 418 (1997) 87.
[16] N.P. Huang, M.H. Xu, C.W. Yuan, R.R. Yu, J. Photochem. Photobiol. A: Chem. 108 (1997) 229.
[17] F. Afaq, P. Abidi, R. Matin, Q. Rahman, J. Appl. Toxicol. 18 (1998) 307.
[18] Y. Nakagawa, S. Wakuri, K. Sakamoto, N. Tanaka, Mutat. Res. 394 (1997) 125.
[19] A. Dupre, P. Touron, J. Daste, J. Lassere, J.-L. Bonafe, R. Viraben, Arch. Dermatol. 121 (1985) 656.
[20] S.A.C. Dundas, R.W. Laing, Dermatologica 176 (1988) 305.
[21] C.A. Moran, F.G. Mullick, K.G. Ishak, F.B. Johnson, W.B. Hummer, Hum. Pathol. 22 (1991) 450.
[22] M.H. Tan, C.A. Commens, L. Burnett, P.J. Snitch, Australas. J. Dermatol. 37 (1996) 185.
[23] World Health Organization, "Sunscreens", IARC Handbooks of Cancer Prevention, vol. 5, 2001. International Agency for Research on Cancer, 150 cours Albert Thomas, 69372 Lyon, France.
[24] R.G. van der Molen, F. Spies, J.M. van't Noordende, E. Boelsma, A.M. Mommaas, H.K. Koerten, Arch. Dermatol. Res. 289 (1997) 514.
[25] A.-S. Dussert, E. Gooris, S. Hemmerle, Int. J. Cosmet. Sci. 19 (1997) 119.
[26] F. Menzel, T. Reinert, J. Vogt, T. Butz, Nucl. Instrum. Meth. Phys. Res. B: Beam Inter. Mater. Atoms 219–220 (2004) 82.
[27] C. Bennat, C.C. Muller-Goymann, Int. J. Cosmet. Sci. 22 (2000) 271.
[28] J. Lademann, H.-J. Weigmann, C. Rickmeyer, H. Barthelmes, H. Schaefer, G. Mueller, W. Sterry, Skin Pharmac. Appl. Skin Physiol. 12 (1999) 247.
[29] R.M. Brand, J. Pike, R.M. Wilson, A.R. Charron, Toxicol. Ind. Health 19 (2003) 9.
[30] R. Cai, K. Hashimoto, K. Itoh, Y. Kobota, A. Fujishima, Bull. Chem. Soc. Jpn. 64 (1991) 1268.
[31] N. Serpone, A. Salinaro, A.V. Emeline, S. Horikoshi, H. Hidaka, in preparation.
[32] M. Gulston, Ph.D. thesis, Oxford University, Department of Biochemistry, 1999.
[33] C. Bignozzi, University of Ferrara, personal communication to N. Serpone, 1997.
[34] We thank Dr. John Knowland, Department of Biochemistry, Oxford University, Oxford, UK, for providing us with the specimen.
[35] T. Maniatis, E.F. Fritsch, J. Sambrook, Molecular Cloning: A Laboratory Manual, Cold Spring Harbor Laboratory, Cold Spring Harbor, N.Y., 1982.
[36] J. Knowland, E.A. McKenzie, P.J. McHugh, N.A. Cridland, FEBS Lett. 324 (1993) 309.
[37] O. Ostling, K.J. Johanson, Biochem. Biophys. Res. Commun. 123 (1984) 291.
[38] N.P. Singh, M.T. McCoy, R.R. Tice, E.L. Schneider, Exp. Cell. Res. 175 (1988) 184.
[39] H.J. Reavy, N.J. Traynor, N.K. Gibbs, Photochem. Photobiol. 66 (1997) 368.
[40] D. Frolov, D. Bavykin, E. Savinov, Catal. Lett. 86 (2003) 169.
[41] Y. Nosaka, Proceedings of the NIMS-2 International Conference on Photocatalysis—Fundamental and Applications, Abstract IV-25, Shonan Village Center, Hayama, Kanagawa, Japan, 1–3 February, 2004.
[42] (a) P.S. Pappas, R.M. Fischer, J. Paint Technol. 46 (1974) 65;
(b) G. Munuera, A. Navio, V. Rives-Arna, J. Chem. Soc. Faraday Trans. 1 77 (1981) 2747;
(c) K. Gohre, G.C. Miller, J. Chem. Soc. Faraday Trans. 1 81 (1985) 793;
(d) R. Konaka, E. Kasahara, W.C. Dunlap, Y. Yamamoto, K.C. Chien, M. Inoue, Free Radical Biol, Med. 27 (1999) 294;
(e) Y. Yamamoto, N. Imai, R. Mashima, R. Konaka, M. Inoue, W.C. Dunlap, Methods Enzymol. 319 (2000) 29;
(f) R. Konaka, E. Kasahara, W.C. Dunlap, Y. Yamamoto, K.C. Chien, M. Inoue, Redox Rep. Commun. Free Radical Res. 6 (2001) 319.
[43] N. Serpone, A. Salinaro, A.V. Emeline, S. Horikoshi, H. Hidaka, J. Zhao, Photochem. Photobiol. Sci. 1 (2002) 970.
[44] D. Dondi, A. Albini, N. Serpone, in preparation.
[45] (a) Z. Huang, P.-C. Maness, D.M. Blake, E.J. Wolfrum, S.L. Smolinski, W.A. Jacoby, J. Photochem. Photobiol. A: Chem. 130 (1999) 163;
(b) P.-C. Maness, S. Smolinski, D.M. Blake, Z. Huang, E.J. Wolfrum, W.A. Jacoby, Appl. Environ. Microbiol. 65 (1999) 4094.
[46] T. Matsunaga, R. Tomoda, T. Nakajima, H. Wake, FEMS Microbiol. Lett. 29 (1985) 211.
[47] D.M. Blake, P.C. Maness, Z. Huang, E.J. Worfrum, J. Huang, Separat. Purific. Methods 28 (1999) 1.
[48] M. Gulston, J. Knowland, Mutat. Res. 444 (1999) 49.
[49] E. Damiani, L. Greci, R. Parsons, J. Knowland, Free Rad. Biol. Med. 26 (1999) 809.
[50] P.J. McHugh, J. Knowland, Photochem. Photobiol. 66 (1997) 276.